

# Non-resonant Optical Injection Locking in Quantum Cascade Laser Frequency Combs

Alexandre Parriaux,<sup>1,\*</sup> Kenichi N. Komagata,<sup>1,3</sup> Mathieu Bertrand,<sup>2</sup>  
Mattias Beck,<sup>2</sup> Valentin J. Wittwer,<sup>1</sup> Jérôme Faist,<sup>2</sup> and Thomas Sudmeyer<sup>1</sup>

<sup>1</sup>*Laboratoire Temps-Frquence, Institut de Physique, Universit de  
Neuchtel, Avenue de Bellevaux 51, 2000 Neuchtel, Switzerland*

<sup>2</sup>*Institute for Quantum Electronics, ETH Zurich, Auguste-Piccard-Hof 1, 8093 Zurich, Switzerland*

<sup>3</sup>*Present address: Nanofiber Quantum Technologies, Inc., 1-22-3 Nishiwaseda, Shinjuku-ku, 169-0051 Tokyo, Japan*

(Dated: December 16, 2024)

Optical injection locking of the repetition frequency of a quantum cascade laser frequency comb is demonstrated using an intensity modulated near-infrared light at 1.55  $\mu\text{m}$  illuminating the front facet of the laser. Compared to the traditional electrical modulation approach, the introduced technique presents benefits from several perspectives such as the availability of mature and high bandwidth equipment in the near-infrared, circumvent the need of dedicated electronic components for the quantum cascade laser, and allows a direct link between the near and mid-infrared for amplitude to frequency modulation. We show that this stabilization scheme, used with a moderate near-infrared power of 5 mW, allows a tight lock to a radio-frequency generator with less than 1 mrad residual phase noise at 1 s integration time. We also perform a full characterization of the mechanism and evidence that the locking range follows Adler's law. A comparison with our recent characterization of the traditional method indicates that the optical approach could potentially lead to lower phase noise, which would benefit mid-infrared spectroscopy and metrological applications.

## I. INTRODUCTION

Frequency combs, i.e, coherent sets of equally spaced discrete optical frequency lines, can be generated with a variety of sources [1], such as mode-locked lasers [2], micro-resonators [3] or electro-optic modulators [4]. In the mid-infrared (MIR), combs sources are scarcer and this spectral region is usually reached via nonlinear frequency conversion from the near-infrared (NIR) [5–7]. However, a few candidates like quantum cascade lasers (QCL) are able to generate a frequency comb directly in the MIR [8, 9], and these particular lasers present unique properties such as a low footprint, high repetition frequencies, watt-level output power [10], potential for mass production, etc. This makes them particularly interesting in several applications such as high resolution spectroscopy [11, 12], time resolved spectroscopy [13], free-space communications [14] or biomedical spectroscopy [15].

Nonetheless, as with other lasers, QCLs are subject to noise types of several origins which can be linked to their structure [16], and the temperature of operation and the related internal fluctuations [17, 18], to only cite a few examples. This degrades the high spectral purity of single-frequency QCLs and limits their use for most applications as mentioned above. Combs generated by QCLs (QCL-comb) suffer from similar problems [8, 19, 20], which means that to improve performance, stabilization procedures are required on both degrees of freedom of the comb, namely the repetition frequency  $f_{\text{rep}}$  and the offset frequency  $f_0$ . For a MIR QCL-comb, the latter is technically difficult to detect directly via standard  $f - 2f$

interferometry [21, 22] due to low peak power generated by QCLs that prevents nonlinear broadening. However, several schemes addressed this issue by bringing a fully stabilized comb in the spectral region of the QCL-comb allowing its full referencing [23, 24], or by using a MIR molecular reference [11].

As for the stabilization of  $f_{\text{rep}}$ , several possibilities are available such as actuation on the current driving the laser in a phase lock loop [20], electrical radio-frequency injection locking (RFIL) [25–27] or actuation using off-resonant light [28]. Note that recent works demonstrated passive stabilization of the repetition frequency using optical feedback [29, 30], however this approach does not reference  $f_{\text{rep}}$  to a radio-frequency (RF) standard. Although the first possibility (drive current actuation) is the most straightforward, it was demonstrated that phase locking the repetition frequency to a RF standard induces an increase in the noise of the comb lines [20]. Regarding electrical RFIL, this technique requires dedicated electrical components for the QCL, and we also recently showed limits in the faithful reproduction of the master oscillator through electrical RFIL [31]. This calls for exploring and carefully characterizing different stabilization methods. In our previous study [32], we showed that NIR light illumination could be one of these new possibilities.

Here, we present the optical RFIL of the repetition frequency in a QCL-comb using a non-resonant, intensity modulated NIR laser illuminating the front facet of the QCL. We characterize the efficiency of the approach in terms of locking range and spectral purity, as a function of injected power. In parallel we also investigate several properties of the QCL-comb under NIR light illumination to fully characterize the impact of its use.

\* Corresponding author: [alexandre.parriaux@unine.ch](mailto:alexandre.parriaux@unine.ch)

## II. EXPERIMENTAL SETUP

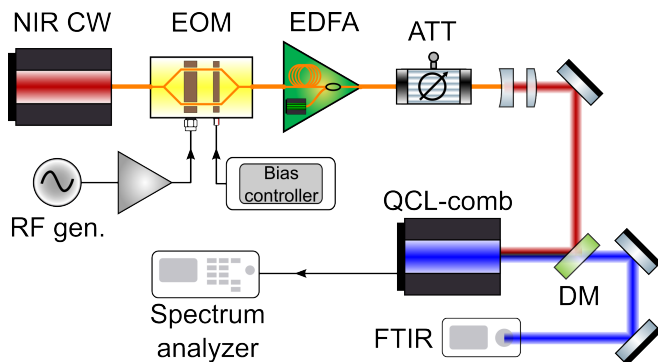


FIG. 1. Schematic showing the experimental setup used for optical RFIL of the repetition frequency of the QCL-comb using an intensity modulated NIR light illuminating the front facet of the QCL, and for characterizing the comb properties. ATT: variable attenuator, DM: dichroic mirror.

Our experimental setup is divided into two parts and schematized in [Figure 1](#). The first one starts with the generation of a MIR frequency comb centered around  $1323\text{ cm}^{-1}$  with a  $45\text{ cm}^{-1}$  bandwidth using a QCL driven at 1020 mA and temperature stabilized at  $2^\circ\text{C}$ . The QCL-comb beam is then collimated with a 1.868 mm focal-length aspheric lens and transmitted through a home-made  $1.55\text{ }\mu\text{m}/7.8\text{ }\mu\text{m}$  dichroic mirror produced with an ion beam sputtering machine. The spectrum of the QCL-comb is monitored using a Fourier-transform infrared spectrometer (FTIR, Bristol 771), and its optical power with a thermal sensor (Thorlabs, S401C). The repetition frequency of the QCL-comb  $f_{\text{rep}}$  is measured thanks to wires placed on top of the QCL-chip that allows to capture the associated voltage originating from the modes beating in the Fabry-Perot cavity [33, 34]. The signal of the electrically extracted beatnote is then characterized using a phase noise analyzer (Rohde & Schwarz, FSWP26) that allows us to analyze the RF spectrum and the phase noise power spectral density (PN-PSD) of  $f_{\text{rep}}$ . With this, one can study the performance of the locking scheme that will be introduced shortly after.

The second part of our setup consists of an intensity modulated and amplified NIR laser that illuminates the front facet of the QCL. Compared to our previous studies [31, 32], the characteristics of the NIR light are adapted to perform optical RFIL of the QCL-comb repetition frequency  $f_{\text{rep}}$ . For this, we use a typical telecommunication laser diode emitting a continuous wave (CW) around  $1.55\text{ }\mu\text{m}$  with 40 mW of optical power. The CW laser is then intensity modulated with a 20 GHz electrical bandwidth electro-optic modulator (EOM) (ixblue, MXAN-LN-20) electrically driven by a signal generator at a frequency  $f_{\text{gen}}$  (Rohde & Schwarz, FSWP26). The bias voltage of the EOM is set at its quadrature point and stabilized using a commercially available bias controller (ixblue, MBC-AN-LAB-A1). The RF power used

to drive the EOM is set at 20 dBm which maximizes the power of the RF signal seen by a photodiode when detecting the optical output of the EOM. This value of RF power will be kept identical throughout the studies presented here. Then, the modulated optical signal is amplified up to 70 mW using a home-made erbium doped fibered amplifier (EDFA), and the resulting signal is connected to a variable attenuator to control the optical power that will further illuminate the front facet of the QCL. Note that NIR powers measured and presented in this article are average powers. The NIR light is then sent to free space via a fibered collimator, and before reaching the home-made  $1.55\text{ }\mu\text{m}/7.8\text{ }\mu\text{m}$  dichroic mirror introduced previously, we focus the beam using a 300 mm focal-length lens. The dichroic mirror is used in reflection for the NIR beam which is then directed to illuminate the front facet of the QCL with a beam diameter slightly below  $20\text{ }\mu\text{m}$ . Note that a smaller beam size could be obtained with different optics to increase the NIR intensity delivered on the QCL front facet.

## III. INJECTION LOCKING CHARACTERIZATION

### A. Response of the QCL with high power illumination

In our previous article [32], we studied the response of several parameters of the QCL when a low power NIR light illuminated its front facet and we showed that the NIR beam alignment was important. Here, as we take an interest in the stabilization of  $f_{\text{rep}}$ , the alignment of the NIR beam on the QCL front facet is made so as to maximize the frequency detuning of  $f_{\text{rep}}$  induced by the NIR illumination. We observed that this is directly linked to the maximization of the electrical voltage  $V$  driving the QCL and several other features (see below). With such an alignment, the variation of  $f_{\text{rep}}$  with respect to the illuminated NIR power  $P_{\text{NIR}}$  can be studied and is presented in [Figure 2 \(a\)](#). A comparison with an adjusted function shows that the frequency detuning induced by the NIR light closely follows a square root trend of the NIR power.

In a similar way, and using a thermal sensor, we monitored the optical power emitted by the QCL when illuminated with our NIR light. The MIR power evolution with respect to  $P_{\text{NIR}}$  is shown in [Figure 2 \(b\)](#), and a comparison of the experimental data with an adjusted function shows a square root function trend as well. As for the repetition frequency detuning, we also observed here that the alignment of the NIR beam on the front facet of the QCL is important, and that the MIR power at a given NIR power is minimized when the driving voltage of the QCL is maximized by NIR light illumination. The trend predicts a complete shutdown of the laser at 60 mW, which is an interesting feature as it could pave the way towards MIR pulse generation with QCLs by us-

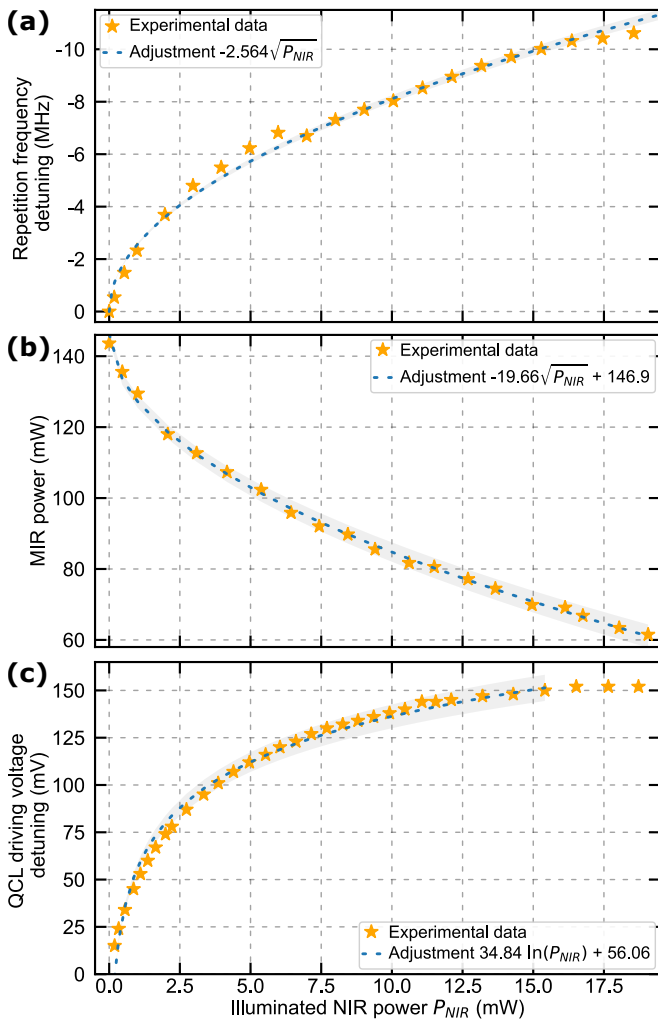


FIG. 2. Graph showing several parameters of the QCL-comb when illuminated with NIR light, and comparisons with adjusted functions. (a) Repetition frequency detuning. Here the zero frequency detuning corresponds to 11.0601 GHz. (b) MIR optical power delivered by the QCL. (c) Change in voltage measured at the bounds of the QCL. The zero voltage change corresponds to a driving voltage of 11.639 V and the driving current was kept at 1020 mA. For all sub-figures, the gray shaded areas represent the two standard deviation margin on the parameters estimated numerically.

ing the NIR light as the handle to intensity modulate the QCL optical output. Pulse generation in the MIR is a hot topic [35, 36], but outside the scope of this paper.

Since the evolution of the QCL repetition frequency  $f_{\text{rep}}$  and optical power with respect to  $P_{\text{NIR}}$  are related to changes in the voltage driving the QCL (at a fixed current), we also studied its evolution in the same NIR beam alignment configuration as above. This is shown in Figure 2 (c) and two different regimes can be observed. First, a saturation effect occurs starting at 17 mW of NIR illuminated power. Second, data analysis shows that, in the non saturated regime, the induced voltage closely follows a logarithm trend.

The behavior of the QCL and the trends observed above when illuminated with high power NIR light is not simple to interpret without performing numerical simulations that investigate the interaction between the QCL and the NIR light, which is beyond the scope of this paper. However, we note that the trends put into evidence here for  $f_{\text{rep}}$ , the MIR optical power, and the driving voltage were also observed for other QCL-comb chips, which corroborates the general applications of our findings. We also note that the evolution of  $f_{\text{rep}}$  and optical power shows similar square root trends as observed for the optical central frequency evolution of terahertz CW QCLs illuminated with a NIR light as shown in Ref. [37, 38].

## B. Phase noise evolution

Using the EOM, we now modulate the NIR CW laser for injection locking of the repetition frequency, and the procedure is the following. First, using the variable attenuator at the end of the NIR fibered path, we adapt  $P_{\text{NIR}}$  to the desired value. As shown in Figure 2 (a), the natural repetition frequency of the QCL will be shifted and so we set the frequency of the generator  $f_{\text{gen}}$  to this new frequency. When the modulation is turned on, using the phase noise analyzer, we study the RF spectrum and the PN-PSD of  $f_{\text{rep}}$  that is electrically extracted on the dedicated channel of the QCL. Figure 3 (a) presents different PN-PSD of  $f_{\text{rep}}$  at several illuminated NIR power levels. Note that for clarity and readability of the graph, only a few curves are displayed but we performed measurements at the same points as the ones in Figure 2 (a). Also note that we measured the PN-PSD of the RF beat-note delivered by our NIR setup using a fast photodiode and we observed no difference with the PN-PSD of the signal delivered by the generator used to drive the EOM.

In Figure 3 (a), we observe that even with a power as low as 180  $\mu\text{W}$ , injection locking can be performed and reduces the PN-PSD drastically, especially at low frequencies where it is reduced by 80 dB at 1 Hz. When increasing  $P_{\text{NIR}}$  the noise at low frequencies continues to decrease and the lock bandwidth, which is the highest frequency at which the noise is reduced compared to the free running state, increases. To gain more insight, we calculated the integrated phase noise  $\phi_{\text{int}}$  associated to the different PN-PSD measurements performed and plotted it against the NIR illumination power, which is shown in Figure 3 (b). A comparison of the experimental data with an adjusted function shows that  $\phi_{\text{int}}$  decreases following an inverse function trend with respect to  $P_{\text{NIR}}$ . Hence, higher illumination power is not linked to a large improvement of the PN-PSD, which motivated our choice to stop power studies around 19 mW of illuminated power. Moreover, one should note that even if  $P_{\text{NIR}}$  can be increased, at a certain point our QCL-comb often started to jump to a different mode, which is associated to radical changes in the optical spectrum and  $f_{\text{rep}}$  and hence detrimental for coherent analysis of the

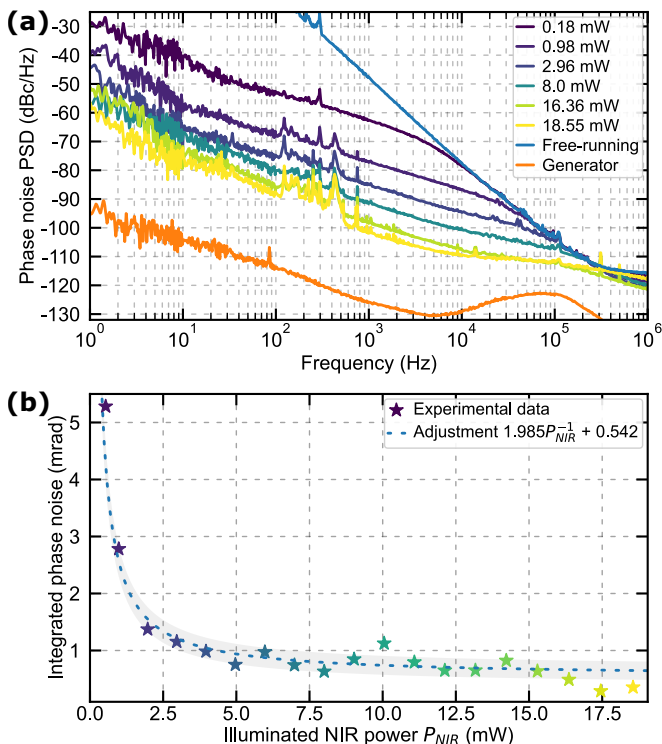


FIG. 3. (a) PN-PSD of the QCL-comb repetition frequency when injection locked using a modulated NIR light illuminating its front facet. (b) Integrated phase noise related to the PN-PSD curves in (a) and other measurements versus the NIR illuminated power  $P_{NIR}$ . The gray shaded area in (b) represents the two standard deviation margin on the parameters estimated numerically.

results. A last remark is that the oscillatory feature observed in Figure 3 (b) is due to the noise contribution between 1 Hz and 10 Hz which impacts the most on the integrated phase noise value, and that can easily vary in minutes long measurements due to mechanical vibrations. Better packaging and thermal regulation of the QCL could reduce and even suppress this effect.

Another interesting feature with this injection locking technique is that the frequency of the generator driving the EOM can be set to half or twice the natural repetition frequency of the QCL-comb. In both cases, we observed only small changes in the PN-PSD of the locked  $f_{rep}$  compared to the case where the frequency of the generator matches  $f_{rep}$ . We believe that these small variations originate from the non-constant electrical response of our setup over the whole range  $\frac{1}{2}f_{rep}$  to  $2f_{rep}$  which is more than 16 GHz. Note that this can easily be compensated by a small adjustment of  $P_{NIR}$ . Although no improvements are observed, this feature can still be useful for designing a cost effective setup as the frequency bandwidth required for the whole NIR setup can be reduced by a factor of 2. Exploring different multiplication or division factors is an interesting topic, but it would deserve a dedicated study.

To better apprehend the results and the impact of us-

ing optical RFIL, we can compare the performance obtained with the electrical RFIL approach. This is however a difficult task as no similar work has been reported in the literature for the reasons we explained in Ref. [31]. Still, some works evidenced limits of electrical RFIL which we can hereby address for a comparison with optical RFIL, especially with our previous study as we used the same QCL. These limits, observed in Refs. [23, 31], first concerns a bump above 1 kHz in the PN-PSD of different comb lines under investigation. As stated in these two works, the bump is related to the comb mode spacing properties as it evolves with the line number. In the case of optical RFIL, the results displayed in Figure 3 (a) do not show such a feature, which seems to indicate that optical RFIL has a better locking bandwidth property. Second, as suggested in Ref. [31], the reproduction of the noise characteristics of the injected oscillator with electrical RFIL seems to be limited to a few kHz offset frequency and with an inverse frequency trend. In the case of optical RFIL, we also observe a similar trend but the frequency limit seems to be at least one order of magnitude above as can be seen in Figure 3 (a) from the stagnancy of the PN-PSD around 50 kHz at the highest NIR light power.

Hence, the presented results suggest that optical RFIL is superior than electrical RFIL in terms of achievable phase noise reduction. One of the potential explanation is that compared to electrical RFIL, optical RFIL is less affected by any electrical impedance mismatch when injecting the RF signal. However, we remain cautious with this claim since the accurate measurement of residual phase noise in the case of electrical RFIL has only been recently demonstrated and not optimized over a broad range of parameters as with the current study. Further studies such as the analysis of the electric field emitted by a QCL stabilized with electrical RFIL or optical RFIL could settle down this issue [24].

### C. Locking range

One last feature that we studied regarding optical RFIL of  $f_{rep}$  is the locking range with respect to the NIR illumination power, which is defined as the frequency range  $\Delta f$  where injection locking is possible. For this, we linearly swept the frequency of the RF generator  $f_{gen}$  used to modulate the NIR light around the natural  $f_{rep}$  of the QCL-comb, and we recorded 200 RF spectra at the output of the RF extraction channel of the QCL-comb to cover the frequency sweep. Figure 4 shows an example of map obtained for a NIR illumination power of 6 mW where three regimes can be observed.

The first regime corresponds to the case where  $f_{gen}$  is relatively far away from the natural repetition frequency of the QCL-comb, and in this case  $f_{rep}$  stays unchanged compared to no modulation of the NIR light. When  $f_{gen}$  is brought closer to  $f_{rep}$ , a pulling mechanism appears such as  $f_{rep}$  is attracted by  $f_{gen}$  and its frequency is hence



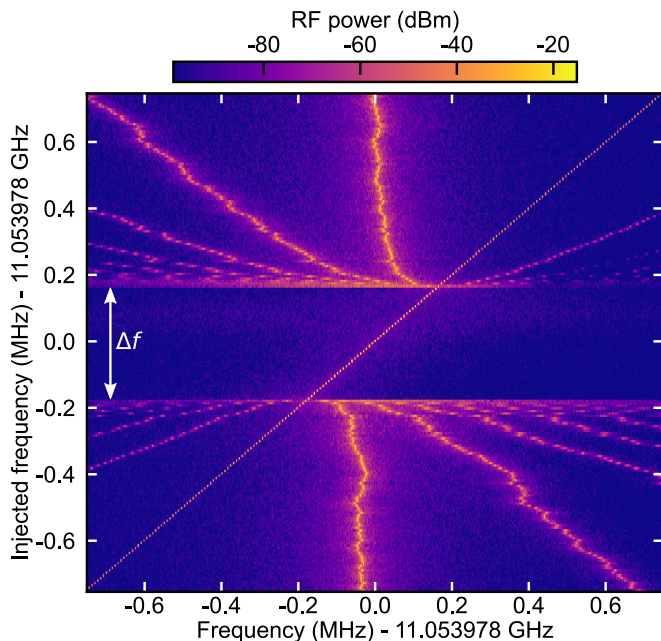


FIG. 4. Set of RF spectra obtained with a resolution bandwidth of 1 kHz at the electrical extraction channel of the QCL when sweeping the frequency of the generator (diagonal line) to observe the bandwidth  $\Delta f$  where the repetition frequency locking occurs. The NIR light power illuminating the front facet of the QCL was set to 6 mW.

modified compared to the case where the NIR light is not modulated. Finally, the last regime is the injection locked regime where  $f_{\text{rep}} = f_{\text{gen}}$  over the locking range  $\Delta f$ . This particular evolution of  $f_{\text{rep}}$  with respect to  $f_{\text{gen}}$  sweeping is characteristic of Adler's formalism of coupled oscillators [39, 40].

We now take an interest of the dependency of the locking range  $\Delta f$  with respect to the NIR illuminated power  $P_{\text{NIR}}$ . For this, we record different maps such as the one presented in Figure 4 at different NIR powers and we extract  $\Delta f$ . The results are displayed in Figure 5 and a numerical adjustment of the experimental data shows that  $\Delta f$  closely follows a linear trend with respect to  $P_{\text{NIR}}$ . This feature is also in accordance with Adler's formalism. Indeed, as we have seen it before and especially in Figure 2 (c), the NIR light illuminating the QCL front facet induces a voltage  $V$  at its bounds, which is related to a RF power  $P_{\text{RF}}$  effectively seen by the QCL such as

$$P_{\text{RF}} = \frac{V^2}{|Z|} \propto P_{\text{NIR}}^2 \quad (1)$$

where  $Z$  is the impedance of the QCL-system. Hence,  $\Delta f$  follows a linear trend with respect to  $P_{\text{NIR}}$  but a square root trend with respect to  $P_{\text{RF}}$ , which is predicted by Adler's formalism [39, 40].

Regarding the alignment of the NIR beam, which we hereby chose so as to maximize the frequency excursion of  $f_{\text{rep}}$  at a given NIR power and hence the voltage  $V$  induced at the bounds of the QCL, we investigated the

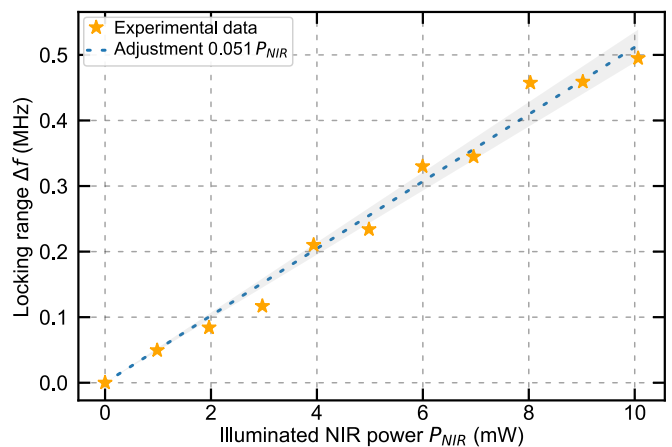


FIG. 5. Graph showing the locking range  $\Delta f$  measured with respect to the NIR light illuminated power. Every experimental point was extracted from the recording of maps such as the one presented in Figure 4. The gray shaded area represents the two standard deviation margin on the parameter estimated numerically.

locking range in different alignment configurations. For a relevant comparison,  $P_{\text{NIR}}$  was kept identical, and the misalignments were chosen so as to induce a similar repetition frequency detuning. In this case, the locking range obtained between four different misalignments was found to be similar but well below the one that could be obtained by maximizing the excursion of  $f_{\text{rep}}$ . On the contrary, for a given shift of  $f_{\text{rep}}$  that is obtained for different values of  $P_{\text{NIR}}$  in different alignments of the NIR beam, we observed similar locking ranges. Hence, optimization of the locking range has to be performed in consistency with all of these aspects, i.e a high NIR power and by maximizing the detuning excursion of  $f_{\text{rep}}$ .

#### D. Optical spectral properties

In parallel to the characterization of the repetition frequency, we also investigated the evolution of the optical spectrum delivered by the QCL with respect to  $P_{\text{NIR}}$  when optical RFIL is performed. Figure 6 shows the spectrum retrieved using a FTIR at three different values of  $P_{\text{NIR}}$ . Note that the spectrum at zero NIR illumination power shows no difference with the one observed at the lowest power of 0,18 mW. One can first observe that the signal-to-noise ratio decreases with  $P_{\text{NIR}}$ , which is linked to the evolution of the MIR power as we have seen it before with Figure 2 (b). The second observation is that the center frequency of the spectrum is slightly pushed towards higher frequencies when increasing  $P_{\text{NIR}}$ , which is in agreement with previous work performed on CW QCLs emitting in the terahertz [37, 38]. Moreover, we observed a similar behavior when operating our MIR QCL in a single operation mode which can be done by setting the pump current at a lower value. Finally, at

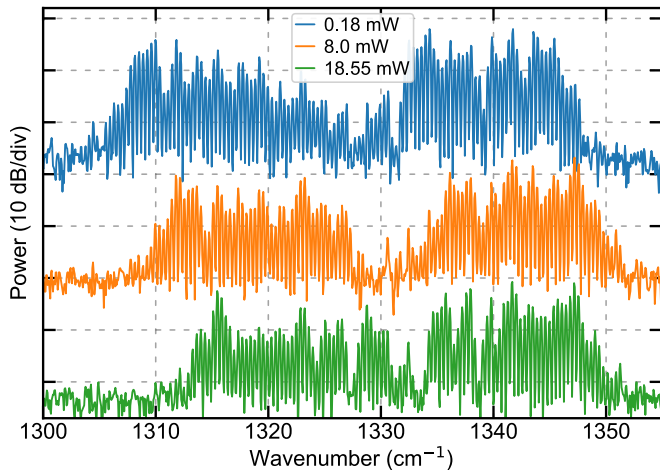


FIG. 6. Graph presenting several optical spectra recorded at different NIR illumination power when injection locking of the repetition frequency of the QCL-comb is performed.

high illumination power, a small reduction of the bandwidth of the comb is observed with around 20 vanishing lines that are mostly located in the red part of the spectrum.

#### IV. DISCUSSION AND CONCLUSION

Stabilization of the repetition frequency of QCL-combs can be performed in various ways, and here we demonstrated a new possibility that requires no feedback loop using an intensity modulated NIR light illuminating the front facet of the QCL. We showed that with a NIR power as low as 180  $\mu$ W, optical RFIL can lead to a strong noise reduction of the repetition frequency, resulting in a tight locking to the generator used. Increasing the NIR power to 5 mW allowed us to reach a residual phase noise below the symbolic value of 1 mrad without decreasing too much the MIR optical power emitted by the QCL nor by modifying too much the comb spectrum. We also observed here that the locking range of the stabilization scheme linearly follows the NIR power illuminating the front facet of the QCL, which is in good accordance with Adler's formalism.

Further investigation on this injection locking mechanism with NIR light illumination is possible, especially on the optical properties of the locked comb. For instance,

SWIFT interferometry can be performed for coherence studies across the spectrum as already made for electrical RFIL [26, 27]. One could also consider studying the comb linewidth by heterodyne beating with a fully stabilized comb [23, 24, 41] to evidence the effect of electrical RFIL and optical RFIL on the noise correlations between  $f_{\text{rep}}$  and  $f_0$  [20]. This could also provide a full comparison between optical RFIL and electrical RFIL, to assess their performance. A demonstration of full stabilization of the QCL-comb using NIR light would also be an interesting study. Regarding the non-resonant light used for injection locking, using a different wavelength in the NIR could offer better performance, e.g., loosen the constraint between noise reduction and MIR power loss. Moreover, the NIR beam delivery could be modified for a better coupling in the QCL and hence reducing the needed NIR power, which could be done by rear facet illumination using an optical fiber brought very close to the QCL chip [38]. Also, one could consider injection at harmonics of the QCL-comb optical central frequency. Finally, we remind that we observed an interesting characteristic of the QCL optical power when the laser chip is illuminated with high power NIR light. As previously described, this could enable pulse generation in the MIR by intensity modulating the QCL using only the NIR light as optical handle. A dedicated study would be needed to fully understand the impact and feasibility of pulse generation using this method.

#### ACKNOWLEDGMENTS

We thank F. Kapsalidis for processing the QCL layer grown and J. Hillbrand for mounting the QCL-chip.

We acknowledge funding from the Schweizerischer Nationalfonds zur Förderung der Wissenschaftlichen Forschung (Grant No. 40B2-1\_176584).

#### AUTHOR DECLARATION

The authors have no conflicts to disclose.

#### DATA AVAILABILITY

The data that support the findings of this study will be openly available in EUDAT B2SHARE at [10.23728/b2share.e9b145dd968b4a3a957f9cdb91d84a65](https://doi.org/10.23728/b2share.e9b145dd968b4a3a957f9cdb91d84a65)

- 
- [1] T. Fortier and E. Baumann, 20 years of developments in optical frequency comb technology and applications, *Communications Physics* **2**, 153 (2019).  
 [2] J. Kim and Y. Song, Ultralow-noise mode-locked fiber lasers and frequency combs: Principles, status, and appli-

- cations, *Advances in Optics and Photonics* **8**, 465 (2016).  
 [3] A. Pasquazi, M. Peccianti, L. Razzari, D. J. Moss, S. Coen, M. Erkintalo, Y. K. Chembo, T. Hansson, S. Wabnitz, P. Del'Haye, X. Xue, A. M. Weiner, and R. Morandotti, Micro-combs: A novel generation of op-

- tical sources, *Physics Reports* **729**, 1 (2018).
- [4] A. Parriaux, K. Hammani, and G. Millot, Electro-optic frequency combs, *Advances in Optics and Photonics* **12**, 223 (2020).
- [5] J. Sotor, T. Martynkien, P. G. Schunemann, P. Mergo, L. Rutkowski, and G. Soboń, All-fiber mid-infrared source tunable from 6 to 9  $\mu\text{m}$  based on difference frequency generation in OP-GaP crystal, *Optics Express* **26**, 11756 (2018).
- [6] Z. Chen, T. W. Hänsch, and N. Picqué, Mid-infrared feed-forward dual-comb spectroscopy, *Proceedings of the National Academy of Sciences* **116**, 3454 (2019).
- [7] N. Hoghooghi, S. Xing, P. Chang, D. Lesko, A. Lind, G. Rieker, and S. Diddams, Broadband 1-GHz mid-infrared frequency comb, *Light Sci. Appl.* **11**, 264 (2022).
- [8] A. Hugi, G. Villares, S. Blaser, H. C. Liu, and J. Faist, Mid-infrared frequency comb based on a quantum cascade laser, *Nature* **492**, 229 (2012).
- [9] J. Faist, G. Villares, G. Scalari, M. Rösch, C. Bonzon, A. Hugi, and M. Beck, Quantum Cascade Laser Frequency Combs, *Nanophotonics* **5**, 272 (2016).
- [10] P. Jouy, J. M. Wolf, Y. Bidaux, P. Allmendinger, M. Mangold, M. Beck, and J. Faist, Dual comb operation of  $\lambda \sim 8.2 \mu\text{m}$  quantum cascade laser frequency comb with 1 W optical power, *Appl. Phys. Lett.* **111**, 141102 (2017).
- [11] K. N. Komagata, M. Gianella, P. Jouy, F. Kapsalidis, M. Shahmohammadi, M. Beck, R. Matthey, V. J. Wittwer, A. Hugi, J. Faist, L. Emmenegger, T. Südmeyer, and S. Schilt, Absolute frequency referencing in the long wave infrared using a quantum cascade laser frequency comb, *Opt. Express* **30**, 12891 (2022).
- [12] J. Hayden, M. Geiser, M. Gianella, R. Horvath, A. Hugi, L. Sterczewski, and M. Mangold, Mid-infrared dual-comb spectroscopy with quantum cascade lasers, *APL Photonics* **9**, 031101 (2024).
- [13] J. L. Klocke, M. Mangold, P. Allmendinger, A. Hugi, M. Geiser, P. Jouy, J. Faist, and T. Kottke, Single-Shot Sub-microsecond Mid-infrared Spectroscopy on Protein Reactions with Quantum Cascade Laser Frequency Combs, *Analytical Chemistry* **90**, 10494 (2018).
- [14] N. Corrias, N. Corrias, T. Gabbrielli, P. D. Natale, L. Consolino, F. Cappelli, and F. Cappelli, Analog FM free-space optical communication based on a mid-infrared quantum cascade laser frequency comb, *Optics Express* **30**, 10217 (2022).
- [15] A. Schwaighofer, M. Brandstetter, and B. Lendl, Quantum cascade lasers (QCLs) in biomedical spectroscopy, *Chemical Society Reviews* **46**, 5903 (2017).
- [16] S. Schilt, L. Tombez, C. Tardy, A. Bismuto, S. Blaser, R. Maulini, R. Terazzi, M. Rochat, and T. Südmeyer, An experimental study of noise in mid-infrared quantum cascade lasers of different designs, *Applied Physics B* **119**, 189 (2015).
- [17] L. Tombez, S. Schilt, J. Di Francesco, P. Thomann, and D. Hofstetter, Temperature dependence of the frequency noise in a mid-IR DFB quantum cascade laser from cryogenic to room temperature, *Opt. Express* **20**, 6851 (2012).
- [18] L. Tombez, F. Cappelli, S. Schilt, G. Di Domenico, S. Bartalini, and D. Hofstetter, Wavelength tuning and thermal dynamics of continuous-wave mid-infrared distributed feedback quantum cascade lasers, *Appl. Phys. Lett.* **103**, 031111 (2013).
- [19] F. Cappelli, G. Villares, S. Riedi, and J. Faist, Intrinsic linewidth of quantum cascade laser frequency combs, *Optica* **2**, 836 (2015).
- [20] A. Shehzad, P. Brochard, R. Matthey, F. Kapsalidis, M. Shahmohammadi, M. Beck, A. Hugi, P. Jouy, J. Faist, T. Südmeyer, and S. Schilt, Frequency noise correlation between the offset frequency and the mode spacing in a mid-infrared quantum cascade laser frequency comb, *Opt. Express* **28**, 8200 (2020).
- [21] D. J. Jones, S. A. Diddams, J. K. Ranka, A. Stentz, R. S. Windeler, J. L. Hall, and S. T. Cundiff, Carrier-envelope phase control of femtosecond mode-locked lasers and direct optical frequency synthesis, *Science* **288**, 635 (2000).
- [22] J. Reichert, M. Niering, R. Holzwarth, M. Weitz, T. Udem, and T. W. Hänsch, Phase coherent vacuum-ultraviolet to radio frequency comparison with a mode-locked laser, *Phys. Rev. Lett.* **84**, 3232 (2000).
- [23] L. Consolino, M. Nafa, F. Cappelli, K. Garrasi, F. P. Mezzapesa, L. Li, A. G. Davies, E. H. Linfield, M. S. Vitiello, P. De Natale, and S. Bartalini, Fully phase-stabilized quantum cascade laser frequency comb, *Nature Communications* **10**, 2938 (2019).
- [24] B. Chomet, S. Basceken, D. Gacemi, B. Schneider, M. Beck, A. Vasanelli, B. Darquié, J. Faist, and C. Sirtori, Heterodyne coherent detection of the electric field temporal trace emitted by frequency-modulated comb lasers, *Optica* **11**, 1220 (2024).
- [25] M. R. St-Jean, M. I. Amanti, A. Bernard, A. Calvar, A. Bismuto, E. Gini, M. Beck, J. Faist, H. C. Liu, and C. Sirtori, Injection locking of mid-infrared quantum cascade laser at 14 GHz, by direct microwave modulation, *Laser Photonics Rev.* **8**, 443 (2014).
- [26] J. Hillbrand, A. M. Andrews, H. Detz, G. Strasser, and B. Schwarz, Coherent injection locking of quantum cascade laser frequency combs, *Nat. Photonics* **13**, 101 (2019).
- [27] B. Schneider, F. Kapsalidis, M. Bertrand, M. Singleton, J. Hillbrand, M. Beck, and J. Faist, Controlling Quantum Cascade Laser Optical Frequency Combs through Microwave Injection, *Laser & Photonics Reviews* **15**, 2100242 (2021).
- [28] L. Consolino, A. Campa, M. De Regis, F. Cappelli, G. Scalari, J. Faist, M. Beck, M. Rösch, S. Bartalini, and P. De Natale, Controlling and phase-locking a THz quantum cascade laser frequency comb by small optical frequency tuning, *Laser Photonics Rev.* **15**, 2000417 (2021).
- [29] C. C. Teng, J. Westberg, and G. Wysocki, Gapless tuning of quantum cascade laser frequency combs with external cavity optical feedback, *Optics Letters* **48**, 363 (2023).
- [30] B. Huang, N. Kosan, and G. Wysocki, Controlled generation of harmonic states in mid-infrared quantum cascade laser frequency combs by external cavity optical feedback, *Optics Express* **32**, 1966 (2024).
- [31] A. Parriaux, K. N. Komagata, M. Bertrand, V. J. Wittwer, J. Faist, and T. Südmeyer, Dual-comb interferometry for coherence analysis of tightly locked mid-infrared quantum cascade laser frequency combs, *Advanced Photonics Research* **5**, 2400006 (2024).
- [32] K. N. Komagata, A. Parriaux, M. Bertrand, J. Hillbrand, M. Beck, V. J. Wittwer, J. Faist, and T. Südmeyer, Coherent control of mid-infrared frequency comb by optical injection of near-infrared light, *APL Photonics* **8**, 086110 (2023).

- [33] M. Rösch, G. Scalari, G. Villares, L. Bosco, M. Beck, and J. Faist, On-chip, self-detected terahertz dual-comb source, *Applied Physics Letters* **108**, 171104 (2016).
- [34] M. Piccardo, D. Kazakov, N. A. Rubin, P. Chevalier, Y. Wang, F. Xie, K. Lascola, A. Belyanin, and F. Capasso, Time-dependent population inversion gratings in laser frequency combs, *Optica* **5**, 475 (2018).
- [35] P. Täschler, M. Bertrand, B. Schneider, M. Singleton, P. Jouy, F. Kapsalidis, M. Beck, and J. Faist, Femtosecond pulses from a mid-infrared quantum cascade laser, *Nat. Photonics* **15**, 919 (2021).
- [36] P. Täschler, L. Miller, F. Kapsalidis, M. Beck, and J. Faist, Short pulses from a gain-switched quantum cascade laser, *Optica* **10**, 507 (2023).
- [37] T. Alam, M. Wienold, X. Lü, K. Biermann, L. Schrottker, H. T. Grahn, and H.-W. Hübers, Wideband, high-resolution terahertz spectroscopy by light-induced frequency tuning of quantum-cascade lasers, *Optics Express* **27**, 5420 (2019).
- [38] T. Alam, M. Wienold, X. Lü, K. Biermann, L. Schrottker, H. T. Grahn, and H.-W. Hübers, Frequency and power stabilization of a terahertz quantum-cascade laser using near-infrared optical excitation, *Optics Express* **27**, 36846 (2019).
- [39] R. Adler, A study of locking phenomena in oscillators, *Proceedings of the IRE* **34**, 351 (1946).
- [40] A. E. Siegman, *Lasers* (University Science Books, 1986) Chap. 29.
- [41] F. Cappelli, G. Campo, I. Galli, G. Giusfredi, S. Bartalini, D. Mazzotti, P. Cancio, S. Borri, B. Hinkov, J. Faist, and P. De Natale, Frequency stability characterization of a quantum cascade laser frequency comb, *Laser Photonics Rev.* **10**, 623 (2016).